Title: *Ins2* gene bursting activity defines a mature β-cell state

Authors: Honey Modi[1], Søs Skovsø[1], Cara Ellis[1], Nicole A.J. Krentz[2], Yiwei Bernie Zhao[3], Haoning Cen[1], Noursadeghi N[1], Evgeniy Panzhinskiy[1], Xiaoke Hu[1], Derek A. Dionne[1], Shouhong Xuan[4], Mark O. Huising[5,6], Timothy J. Kieffer[1], Francis C. Lynn[2], James D. Johnson[1]*

Affiliations:
[1] Diabetes Research Group, Life Sciences Institute, Department of Cellular and Physiological Sciences & Department of Surgery, University of British Columbia, Vancouver, Canada
[2] BC Children's Hospital Research Institute, Department of Surgery, University of British Columbia, Vancouver, Canada
[3] Biomedical Research Centre, Department of Cellular and Physiological Sciences & Department of Surgery, University of British Columbia, Vancouver, Canada
[4] Department of Medicine Hematology and Oncology, Columbia University Medical Center, New York, USA
[5] Department of Neurobiology, Physiology and Behavior, UC Davis, Davis, USA
[6] Department of Physiology and Membrane Biology, UC Davis, Davis, USA

***Address correspondence to:** James D. Johnson, PhD., Faculty of Medicine, Department Cellular and Physiological Sciences, The University of British Columbia, Life Sciences Institute, 5358 – 2350 Health Sciences Mall, Vancouver, British Columbia, Canada V6T 1Z3
Phone: 604 822 7187, Email: James.d.johnson@ubc.ca, Twitter: @JimJohnsonSci

Abstract Word Count: 230
Word Count: 4037
Reference Count: 54
Figure Count: 5
Keywords: Insulin production; cellular heterogeneity; single-cell RNA sequencing, beta-cell fragility
Blurb: Previously reported pancreatic β-cell heterogeneity reflects β-cell state transitions.
Declaration of Interests: The authors declare no competing interests.
Funding: Research was supported by a CIHR operating grant to J.D.J.
Acknowledgments: We thank many colleagues for helpful discussions.
Author Contributions:
HM designed studies, performed experiments, analyzed/interpreted data, and wrote the first draft of the manuscript.
SS performed experiments, analyzed/interpreted data.
CE analyzed/interpreted data.
HC performed experiments, analyzed/interpreted data.
NAJK analyzed/interpreted data.
DAD performed experiments, analyzed/interpreted data.
BX analyzed/interpreted data.
XH performed experiments.
NN performed experiments and analyzed/interpreted data.
EP supervised work and analyzed/interpreted data.
SX provided a key reagent.
MOH provided a key reagent, designed studies, and analyzed/interpreted data.
TJK supervised work.
FCL supervised work and analyzed/interpreted data.
JDJ conceived the project, designed studies, interpreted data, edited the manuscript, and is the guarantor of this work.

Abstract

Heterogeneity within specific cell types is common and increasingly apparent with the advent of single-cell transcriptomics. Transcriptional and functional cellular specialization has been described for insulin-secreting β-cells of the endocrine pancreas, including so-called extreme β-cells exhibiting >2 fold higher insulin gene activity. However, it is not yet clear whether β-cell heterogeneity is stable or reflects dynamic cellular states. We investigated the temporal kinetics of endogenous insulin gene activity using live-cell imaging, with complementary experiments employing FACS and single-cell RNA sequencing, in β-cells from *Ins2*^{GFP} knock-in mice. *In vivo* staining and FACS analysis of islets from *Ins2*^{GFP} mice confirmed that at a given moment, ~25% of β-cells exhibited significantly higher activity at the conserved insulin gene *Ins2*(GFP)^{HIGH}. Live-cell imaging captured on and off 'bursting' behaviour in single β-cells that lasted hours to days. Single cell RNA sequencing determined that *Ins2*(GFP)^{HIGH} β-cells were enriched for markers of β-cell maturity and had reduced expression of anti-oxidant genes. *Ins2*(GFP)^{HIGH} β-cells were also significantly less viable at all glucose concentrations and in the context of ER stress. Collectively, our results demonstrate that the heterogeneity of extreme insulin production, observed in mouse and human β-cells, can be accounted for by dynamic states of insulin gene activity. Our observations define a previously uncharacterized form of β-cell plasticity. Understanding the dynamics of insulin production has relevance for understanding the pathobiology of diabetes and for regenerative therapy research.

Introduction

Pancreatic β-cells in the islets of Langerhans are the only source of circulating insulin, a conserved and essential hormone that is required for nutrient homeostasis and life (Szabat et al., 2016). Insulin production is highly demanding, as insulin mRNA can account for roughly half of all β-cell mRNA and its synthesis, folding and processing require semi-specialized transcription factors, enzymes and cellular conditions. However, not all β-cells appear the same. Indeed, functional β-cell heterogeneity is well established (Benninger and Hodson, 2018), including cellular specialization for islet cell synchronization, insulin secretion, insulin production, and marker gene expression (Bader et al., 2016; Dorrell et al., 2016; Heimberg et al., 1993; Johnston et al., 2016; Kiekens et al., 1992; Kolic and Johnson, 2016; Ling et al., 1998; Pipeleers, 1992; van der Meulen et al., 2017; Wills et al., 2016; Xin et al., 2018). For example, recent *in situ* imaging has revealed the existence of extreme β-cells, defined as having >2 fold *Ins2* mRNA than the median expression as measured by single-molecule fluorescence *in situ* hybridization (Benninger and Hodson, 2018; Farack et al., 2019). Single cell RNA sequencing has shown that human β-cells also express *INS* over a similarly wide range (Xin et al., 2018). However, it remains unclear whether this variation is the hallmark of distinct stable populations of β-cells, or whether it is indicative of transitions between more labile β-cell states.

To date, the vast majority of islet cell 'sub-populations' have been defined by single time-point snapshots, making it impossible to know to what extent observed β-cell heterogeneity represents different islet cell 'fates' or different islet cell 'states'. This information is essential for interpreting existing and future data in the field. Using a dual *Ins1* and *Pdx1* promoter reporter construct and live-cell imaging, we have previously demonstrated that mouse and human β-cells can transition between less and more differentiated states over a time scale of ~24 hours (Szabat et al., 2010; Szabat et al., 2009; Szabat et al., 2011). However, the artificial promoter constructs in these early studies may not reflect endogenous gene activity, leaving open the question of whether endogenous insulin gene activity is similarly dynamic.

In this study, we studied endogenous insulin gene activity using an *Ins2*^{GFP} knock-in/knockout mouse line in which the coding sequencing of the evolutionarily conserved *Ins2*

gene has been replaced with GFP (Wakae-Takada et al., 2013). Live-cell imaging of dispersed cells from *Ins1*^{mCherry}:*Ins2*$^{GFP/wt}$ mice revealed that GFP fluorescence flashed on and off in a subset of cells, suggesting bursts of transcription at the *Ins2* gene locus rather than stable heterogeneity. Single-cell RNA sequencing was used to characterized the *Ins2*(GFP)^{HIGH} cellular state in an unbiased way, revealing increased markers of β-cell maturity as well as alterations in protein synthesis machinery and cellular stress response networks. Pancreatic β-cells in the *Ins2*(GFP)^{HIGH} cellular state were also more fragile across a range of stress conditions. To the best of our knowledge, our observations are the first to define the temporal kinetics of endogenous insulin gene activity, which represents a previously uncharacterized form of β-cell plasticity. Understanding the dynamics of insulin production has relevance for understanding the pathobiology of diabetes and for regenerative therapy research (Johnson, 2016).

Results

In vivo heterogeneity of insulin content in human β-cell and insulin gene activity in Ins2^{GFP} *mice*

Heterogeneity of insulin production is an established phenomenon, and we started our study by staining human pancreas with antibodies to insulin and PDX1, a key transcription factor for β-cell survival and function (Johnson et al., 2003; Szabat et al., 2012). As expected based on single-cell RNA sequencing data (Xin et al., 2018) and previous single-cell imaging of human β-cells (Johnson et al., 2006), imaging over a large dynamic range enabled the identification of β-cells with both high and low insulin protein levels in human pancreas (Fig. 1A). We have previously shown limited correlations between insulin content and Pdx1 immunofluorescence or nuclear localization in human β-cells (Johnson et al., 2006). In order to study insulin gene activity in living cells, we examined islets from mice in which the coding sequencing of the evolutionarily conserved *Ins2* gene has been replaced with GFP (Wakae-Takada et al., 2013)(Fig. 1B). Mice lacking 1 or 2 functional *Ins2* alleles had normal glucose homeostasis (Fig. 1C), consistent with our previous studies of *Ins2* knockout mice (Mehran et al., 2012) and the ability of *Ins1* to compensate (Leroux et al., 2001). Immunofluorescence staining of pancreata from *Ins2*^{GFP} mice revealed a clear bimodal distribution of endogenous insulin production *in vivo* (Fig. 1D). Hand counting 1879 cells across 11 randomly selected islets showed that 38.7% of β-cells had substantially higher GFP immunofluorescence above an arbitrary, but consistently applied, threshold (Fig. 1D). The percentage of cells with high GFP did not appear to vary as a function of islet size. We have observed similar heterogeneity when examining the β-galactosidase knock-in in to the *Ins2* locus (Mehran et al., 2012). Similarly, FACS confirmed this bimodal distribution and that less than half of all β-cells engage in high *Ins2* gene transcription at a given time (Fig. 1E). FACS analysis also validated that GFP mRNA, *Ins2* mRNA, and pre-mRNA were significantly increased in GFP-positive cells compared to negative cells (Fig. 1F,G), strongly suggesting that GFP protein levels accurately reflect *Ins2* mRNA in this system. We did not expect there to be a perfect correlation due to the different predicted transcription-to-protein time courses for GFP and insulin (Fig. 1H; see Supplemental Materials for calculations). Nevertheless, these data demonstrate that GFP production, reflecting the activity of the endogenous *Ins2* gene locus, is bimodal *in vivo* and *ex vivo*, with 25% of β-cells showing significantly higher activity. Hereafter, we refer to cells with high GFP abundance as *Ins2*(GFP)^{HIGH}.

Live-cell imaging of insulin gene activity in Ins2^{GFP}*;Ins1-mCherry mice*

We next crossed the *Ins2*^{GFP} knock-in line with transgenic mice with an allele wherein histone-fused mCherry is driven by the less complex *Ins1* promoter that are known to show relatively stable mCherry fluorescence in virtually all β-cells (Benner et al., 2014), in order to have a model whereby *Ins2* gene activity could be tracked in real-time, while observing all β-

cells. As expected, immunofluorescence of intact pancreatic sections and FACS analysis of dispersed islets from *Ins2*$^{GFP/wt}$:*Ins1*-mCherry mice showed that mCherry labelled virtually all β-cells, while GFP was robustly expressed in a clearly separated sub-set of β-cells we deemed *Ins2*(GFP)^{HIGH} (Fig. 2A,B,C). qPCR of these FACS purified cells confirmed the expected elevated expression of GFP, *Ins2*, pre-*Ins2*, *Ins1*, and pre-*Ins1* mRNA in *Ins2*(GFP)^{HIGH} cells (Fig. 2D). *Ins2* pre-mRNA would be expected to precede GFP fluorescence by at least 1.3 hours, as per estimations in Fig. 1H and calculations in Supplemental Information, which provides a possible explanation for the elevated pre-*Ins2* in the mCherry positive, but GFP low β-cells. Both intact islets and dispersed islet cells isolated from *Ins2*$^{GFP/wt}$:*Ins1*-mCherry mice showed a similar proportion of *Ins2*(GFP)^{HIGH} and *Ins2*(GFP)^{LOW} cells that we observed *in vivo*, demonstrating that this heterogeneity was not altered by isolation or dispersion/culture.

Dispersed islet cells from the resulting double-mutant *Ins2*$^{GFP/wt}$:*Ins1*-mCherry were studied over ~3 days using a high-throughput imaging system with environmental control. Remarkably, live cell imaging identified a sub-set of β-cells that transitioned in and out of *Ins2*(GFP)^{HIGH} activity states over the course of 36-hour long recordings (Fig. 3A). In a pilot study, we did not observe differences in the incidence of this bursting behavior when comparing cells at 3 mM, 5 mM, 10 mM, and 15 mM glucose. We quantified and analyzed 16 cellular behaviour traits in 547 cells for the purpose of clustering them into groups using Cell Profiler software and custom R scripts. We found that 153 out of 547 cells showed dynamic changes in GFP activity (Fig. 3B,C). Principal component analysis identified 3 distinct clusters of *Ins2* gene activity cell behaviours (Fig. 3C,D). Together with our *in vivo* data (Figs. 1,2), these long-term live-cell imaging recordings demonstrate significant dynamic fluctuations in the activity of the endogenous *Ins2* locus in primary β-cells.

Profiling β-cell states with single-cell RNA sequencing

To characterize the *Ins2*(GFP)^{HIGH} state in a comprehensive and unbiased way, we performed single-cell RNA sequencing on FACS purified *Ins2*(GFP)^{HIGH} and *Ins2*(GFP)^{LOW} cells from islets pooled from 3 mice (Fig. 4A,B). We then examined differential gene expression as a function of *gfp* mRNA (Fig. 4C), including only single cells expressing *Ins1* mRNA which are presumably β-cells or rare multi-hormonal islet cells. We also considered *Ins2*(GFP)^{HIGH} and *Ins2*(GFP)^{LOW} as binary categories and obtained similar results (Supplemental Figure S1 A,B).

In 8 week-old *Ins2*$^{GFP/wt}$ mice, gene ontology analysis showed that the *Ins2*(GFP)^{HIGH} cells had significant alterations in genes involved in extracellular matrix, protein synthesis and protein cleavage. Cluster of genes ordered by *gfp* gradient in heterozygous *Ins2*$^{GFP/wt}$ β-cells showed that tetraspanin-28 (*Cd81*) and chromogranin A (*Chga*) that most closely correlated to *gfp* mRNA at the single-cell level. The *gfp*-high state also was characterized by increased mRNA expression of other notable genes encoding transthyretin (*Ttr*) and G-protein subunit gamma 12 (*Gng12*). The *gfp*-high state was associated with decreased expression of genes including soluble factors such as peptide YY (*Pyy*), prodynorphin (*Pdyn*), pancreatic polypeptide (*Ppy*), macrophage inhibitory factor (*Mif*), and *Serpina7*, suggesting in aggregate a less 'poly-hormonal' and therefore, more mature, gene expression profile (Basford et al., 2012; Hrvatin et al., 2014; Johnson, 2016). In agreement with this, *gfp*-high β-cells had lower expression of pappalysin 2 (*Pappa2*), an α-cell-selective regulator of insulin-like growth factor bioavailability, and the epsilon-cell marker (*Etv1*)(Segerstolpe et al., 2016)(Fig. 4D). *Gfp*-high cells also had reduced expression of several genes linked to insulin production and secretion, such as multiple subunits of the 40S and 60S ribosomes, eukaryotic translation initiation factor 3 subunit C (*Eif3c*), eukaryotic translation elongation factor 1 alpha 1 (*Eef1a1*), peptidylglycine alpha-amidating monooxygenase (*Pam*), chromogranin B (*Chgb*), heat shock 70kDa protein 9 (*Hspa9;* Mortalin), G-protein subunit gamma 5 (*Gng5*), regulator of G-protein signaling 4 (*Rgs4*), synaptotagmin 4 (*Syt4*)(Huang et al., 2018; Thomsen et al., 2018)(Fig. 4D). Thus, in young

mice, the *Ins2*(GFP)^{HIGH} cell state is associated with a mature single-cell gene expression profile and a reorganization of protein synthesis machinery.

Age is known to significantly alter the properties of pancreatic β-cells, including their function and ability to enter the cell cycle (Rankin and Kushner, 2009). Thus, we conducted an additional similar study in three 60 week-old mice. In this experiment, we studied cells from both *Ins2*$^{GFP/wt}$ (Fig. 5) and *Ins2*$^{GFP/GFP}$ islets (Fig. S1,S2,S3). Cluster analysis of genes ordered by *gfp* gradient in old heterozygous *Ins2*$^{GFP/wt}$ β-cells revealed that *Neurod1* expression most closely match *gfp* mRNA (Fig. 5C). Other genes that increased with *gfp* expression included genes required for optimal insulin secretion such as chromogranin A (*Chga*), the Glut2 glucose transporter (*Slc2a2*), the insulin granule zinc-transporter (*Slc30a8*), and key β-cell transcription factors and maturity markers *Ucn3* and *Pdx1* (Szabat et al., 2012). Interestingly, many of the mRNAs that were increased are known to be *Pdx1* target genes in islets (Sachdeva et al., 2009). *Gfp*-high cells over-expressed the lncRNA *Meg3*. Other notable genes that were upregulated in Gfp-high cells were G-protein subunit gamma 12 (*Gng12)*, protein phosphatase 1 regulatory inhibitor subunit 1A (*Ppp1r1a*), and metabolism-regulating genes, such as glucose-6-phosphatase catalytic subunit 2 (*G6pc2*), hydroxyacyl-CoA dehydrogenase (*Hadh*), cytochrome C oxidase subunit 6A2 (*Cox6a2*), and a cluster of other mitochondrial genes (Fig. 5C). Also in agreement with the analysis of young islets, gfp-high β-cells from old homozygous mice had decreased expression of *Pappa2*, *Etv1*, and *Chgb* (Fig. 5C), as well as other markers of β-cell immaturity (*Gcg*, *Ppy*, *Pyy*). We observed a reduction the glycolytic enzyme phosphoglycerate mutase 1 (*Pgam1*). Older *gfp*-high β-cells also had reduced expression the apoptosis regulators *Fam162a* and *Bnip3*, the anti-oxidant metallothionein proteins *Mt1* and *Mt2*, glutathione S-transferase omega 1 (*Gsto*), as well as the stress adaptation gene nuclear protein 1 transcriptional regulator *Nupr1*. The stress-induced ER chaperone, heat shock protein family A, member 5 (*Hspa5*; a.k.a. BIP), showed peak expression in moderately *gfp* expressing cells (Fig. 5C), consistent with its known relationship with insulin production in human β-cells (Xin et al., 2018). Heat shock protein 90kDa beta 1 (*Hsp90b1*, a.k.a. Grp94), also an ER-resident protein, had a similar expression pattern to *Hspa5*.

Separately, we analyzed genes ordered by *gfp* mRNA gradient in old homozygous *Ins2*$^{GFP/GFP}$ β-cells (Fig. S2). Many of the same genes that we saw in the heterozygous samples were also increased in the GFP homozygous samples, including *Chga*, *Ucn3*, *Slc2a2*, *Gng12*, and *Ppp1r1a*.

This analysis further revealed the key β-cell maturity transcription factor *Nkx6.1*, creatine kinase B (*Ckb*), and *Ins2* as positively correlated with *gfp* mRNA, that later representing reads mapped to the residual wildtype sequencing remaining after the GFP knock-in (Fig. 1B).

Genes that were anti-correlated with *gfp* mRNA old homozygous *Ins2*$^{GFP/GFP}$ β-cells including 18 genes found in the heterozygous samples (Fig. S2), as well as additional de-differentiation markers (*Sst*, *Ldha*) and the cell cycle regulator, cyclin D1 (*Ccnd1*). Other genes that were reduced in β-cells with high *gfp* expression were glyceraldehyde-3-phosphate dehydrogenase (*Gapdh*), endoplasmic reticulum oxidoreductase 1 alpha (*Ero1l*), regulator of G-protein signaling 4 (*Rgs4*), and heme oxygenase 1 (*Hmox1*). When we combined data from *Ins2*$^{GFP/wt}$ and *Ins2*$^{GFP/GFP}$ cells, gene ontology analysis in the older mouse β-cells showed that the *Ins2*(GFP)^{HIGH} cells had significant alterations in genes involved in nitric oxide mediated signal transduction, insulin secretion, and pancreas development (Fig. 5C). By this analysis, *gfp* expression with many of the same genes found by analysing *Ins2*$^{GFP/wt}$ and *Ins2*$^{GFP/GFP}$ cells separately (Fig. S3).

The single-cell RNA sequencing studies identified enrichment in genes that control β-cell stress responses and markers of β-cell maturity. We have previously shown that insulin production itself is a significant stress under basal conditions in β-cells (Szabat et al., 2016) and we therefore predicted that cells with increased *Ins2* gene activity and GFP production would be

more sensitive to stress. Indeed, *Ins2*(GFP)^{HIGH} cells were >10 fold more sensitive to apoptosis at all glucose concentrations we tested when compared with *Ins2*(GFP)^{LOW} cells in the same cultures (Fig. 6A). Thus, the states marked by high gene activity at the endogenous *Ins2* locus are likely to possess critical functional differences.

Discussion

The goal of the present study was to determine the nature of *Ins2* gene expression heterogeneity. Analysis of pancreatic tissue sections from *Ins2*^{GFP} knock-in mice showed that, at any given time, only about half of all β-cells were robustly GFP-positive, suggesting that not all β-cells have active transcription at the *Ins2* locus *in vivo*. Over the course of multi-day *in vitro* imaging experiments, we observed clear transitions between *Ins2*(GFP)^{HIGH} and *Ins2*(GFP)^{LOW} states in single β-cells. However, *Ins2* gene activity was stable for the duration of these studies in the majority of cells, indicating the typical period of insulin gene activity 'bursting' is greater than 36 hours. We used single-cell RNA sequencing to characterize the *Ins2*(GFP)^{HIGH} cellular state and found that *Ins2*(GFP)^{HIGH} were significantly more sensitive under all stress conditions examined. Together with previous live-cell imaging data, the results of the present study demonstrate that a substantial component of β-cell heterogeneity is dynamic in time (Fig. 6B).

The dynamics of GFP fluorescence revealed by live-cell imaging of dispersed islet cells from *Ins1*-mCherry:*Ins2*$^{GFP/wt}$ mice provided an unprecedented look at insulin gene activity in populations of single β-cells. Many of the *Ins2*(GFP)^{LOW} and *Ins2*(GFP)^{HIGH} β-cell states were maintained over at least 24 hours. We have no evidence that the state transitions were linked to the β-cell circadian clock. Our observation of relatively rapid transitions between *Ins2*(GFP)^{LOW} and *Ins2*(GFP)^{HIGH} β-cell states suggests bursts of transcription at the *Ins2* gene locus rather than stable heterogeneity. However, our measurements of GFP fluorescence originating from *Ins2*-locus mediated transcription cannot distinguish the relative contribution in changes in GFP mRNA transcription/stability or GFP protein translation/degradation. The half-life of unmodified GFP is ~26 hours (Corish and Tyler-Smith, 1999) and the rapid changes in GFP fluorescence in some cells suggest coordinated bursts of protein synthesis and coupled protein degradation.

The study of pancreatic islet cell heterogeneity is currently experiencing resurgence, in part due to the application of single-cell sequencing and optogenetic technologies to islet biology questions. There are many examples of β-cell heterogeneity and these were reviewed recently (Benninger and Hodson, 2018). Insulin gene expression is a cardinal feature of pancreatic β-cells, but cell-by-cell variability in insulin production has remained under-appreciated despite published evidence (Kiekens et al., 1992). For example, there are reports of significant β-cell heterogeneity in transgenic mice expressing GFP under the *Ins2* promoter (Katsuta et al., 2012). Similarly, we have shown variation in fluorescent protein expression under the control of *Ins1* promoters *in vivo* and *in vitro* (Szabat et al., 2010; Szabat et al., 2009; Szabat et al., 2011). However, a limitation in these studies is that artificial promoter constructs may not recapitulate the more complex and long-range regulation available at the endogenous gene locus. Notwithstanding, cell-by-cell analysis of insulin mRNA, either by single-molecule fluorescent *in situ* hybridization or single-cell RNA sequencing, also showed a 2- to 10-fold range in native gene expression from endogenous insulin gene loci (Farack et al., 2019; Xin et al., 2018). The *Ins2*(GFP)^{HIGH} β-cells we identified in our study are likely to be the temporal manifestation of the extreme β-cells reported by Farack et al. Supporting this, and consistent with our single-cell RNA sequencing data, their extreme β-cells had significantly elevated *Chga* mRNA expression (Farack et al., 2019). It is also notable that both extreme β-cells and our *Ins2*(GFP)^{HIGH} β-cells had relatively normal total insulin staining, a clue that further supports the transient nature of bursts in endogenous *Ins2* gene activity. It is possible that the dynamic nature of insulin transcription is an adaptation to the extremely high demands of producing and maintaining adequate stores of insulin in β-cells. Assuming there are homeostatic mechanisms to maintain

stable insulin protein stores, it is unclear how the need for a burst of insulin gene activity would be sensed by individual β-cells. Future studies should attempt to define these mechanisms.

The relationship between β-cell state and disease pathogenesis remains unclear. Isolated islets and single human β-cells from people with type 2 diabetes have reduced *INS* expression on average (Segerstolpe et al., 2016; Yang et al., 2011). Extreme β-cell were significantly more common in diabetic *db/db* mice (Farack et al., 2019). We found that the *Ins2*(GFP)^{HIGH} state was associated with significant vulnerability to cellular stress, so having an excess number of *Ins2*(GFP)^{HIGH} β-cells at a given time may negatively affect islet health and robustness. These results are consistent with our previous data defining the interrelationships between maximal insulin production, ER stress and β-cell proliferation (Szabat et al., 2016). It is also likely that stress may modulate the frequency of these β-cell state transitions, although we did not test this directly. The presence of proportion of β-cells in the *Ins2*(GFP)^{LOW} state may also be essential for islet function. Specifically, so called 'hub β-cells' that help synchronize islets were reported to have lower insulin content compared with typical β-cells (Johnston et al., 2016), and we have speculated that this represents a trade-off needed for their synchronizing function (Kolic and Johnson, 2016). Rodent and human β-cells are long-lived (Perl et al., 2010; Teta et al., 2005), and perhaps β-cells cycle through multiple states during their existence, including taking turns supporting the oscillatory coupling of the islet. Given that robust β-cell heterogeneity and state transitions have not been reported for stem-cell derived β-like cells (Veres et al., 2019), it is likely that *in vitro* differentiation protocols will need to be further optimized to produce a full range of dynamic β-cell characteristics. Interestingly, many of the genes that are differentially expressed in *Ins2*(GFP)^{HIGH} β-cells are known to play roles in type 2 diabetes susceptibility, including common alleles of the MODY/neonatal diabetes genes *Pdx1*, *Neurod1*, *Nkx6.1*, *Abcc8*, *Slc2a2*, as well as *Slc30a8* and *Pam* genome-wide association previously identified by genome-wide association (Thomsen et al., 2018). It will also be interesting to examine the frequency of β-cell states in the context of type 1 diabetes, given that pro-insulin, *Slc30a8* and *Chga* are auto-antigens (Nakayama et al., 2005; Stadinski et al., 2010; Wenzlau et al., 2007). Indeed, β-cells undergoing proliferation or with lower insulin/maturity are protected in the NOD mouse model of type 1 diabetes (Dirice et al., 2019; Rui et al., 2017). Collectively, these observations suggest that modulation of β-cell state could be a therapeutic and/or prevention target for both type 1 diabetes and type 2 diabetes.

Temporal transcriptional plasticity and gene expression bursting on a similar time scale as to what we have observed have been documented in bacteria, yeast and other mammalian cell types (Raj et al., 2006; Suter et al., 2011; Vera et al., 2016). For example, bursting gene expression patterns have been observed in pituitary cells (Harper et al., 2010; Norris et al., 2003; Walsh and Shupnik, 2009). Interestingly, LHβ transcription in pituitary gonadotrophs is directly linked to proteasome activity (Walsh and Shupnik, 2009), suggesting a possible mechanism for coupling protein loads and transcription in secretory cell types. Many cell-extrinsic and cell-intrinsic factors have been implicated in the modulation of transcriptional burst frequency, including histone modifications and chromatin topology(Atger et al., 2015; Molina et al., 2013; Nicolas et al., 2017; Nicolas et al., 2018; Phillips et al., 2019). Future studies will be required to determine the molecular mechanisms mediating transcriptional bursting at the insulin gene locus in β-cells. Future studies should also seek to directly measure *Ins2* mRNA transcription, perhaps using new CRISPR-based probes (Pichon et al., 2018).

In conclusion, our data demonstrate that single β-cells can switch between states marked by high and low activity of the phylogenetically conserved, endogenous insulin gene locus. This newly discovered phenomenon may account for much of the observed β-cell heterogeneity measured at single time points and needs to be comprehensively studied and leveraged in efforts to protect and generate β-cells (Johnson, 2016).

Methods

Animals and in vivo physiology

Ins2$^{GFP/wt}$ knock-in mice were obtained from Shouhong Xuan (Wakae-Takada et al., 2013). These mice were crossed with transgenic mice where the *Ins1* promoter drives a mCherry:H2B fluorescent fusion protein (Benner et al., 2014). Glucose tolerance and insulin secretion were assessed in both male and female mice (12-14 weeks) injected intraperitoneally with 2g/kg (20%) glucose after a 5 hr fast. Insulin from *in vivo* samples was measured using ELISA kits from Alpco (Salem, NH, USA). Insulin tolerance was assessed after injection of 0.75 U insulin per kg body weight after a 5 hr fast.

Immunostaining

Pancreata from PBS perfused mice were harvested and fixed in 4% paraformaldehyde for 24 hr before being washed and stored in 70% ethanol, prior to paraffin embedding. Pancreatic sections (5 µm) were taken from at least three different regions of the pancreas 100 µm apart. Sections were deparaffinized, hydrated with decreasing concentrations of ethanol, and rinsed with PBS. Sections were subjected to 15 min of heat-induced epitope retrieval at 95°C using a 10 mM citrate buffer, pH 6.0. Sections were blocked then incubated with primary antibodies overnight in a humid chamber at 4°C. A list of primary antibodies can be found in Antibodies section. Primary antibodies were visualized following incubation with secondary antibodies conjugated to AlexaFluor 488, 555, 594, or 647 as required (1:1,000; Invitrogen). Counter staining was done by Vectasheild mounting media with DAPI (H-1200). Images for β cell and α cell area were taken on ImageXpress^{MICRO} using a 10× (NA 0.3) objective and analyzed using the MetaXpress software (Molecular Devices Corporation, San Jose, CA, USA). All other images were taken on a Zeiss 200M microscope using 20× air (NA 0.75), 40× oil (NA 1.3), and/or 100× oil (NA 1.45) objectives and analyzed using Slidebook software (Intelligent Imaging Innovations, Denver, CO, USA). For quantification of immunofluorescence we used the segment masking function of Slidebook, generating a GFP high mask and a GFP low mask (by subtracting the GFP high mask from the insulin mask). A list of primary antibodies can be found in Table S1.

Islet isolation and culture

Pancreatic islets were isolated using collagenase, filtration, and hand-picking as described (Szabat et al., 2010). Islets were cultured overnight (37°C, 5% CO_2) in RPMI1640 medium (Invitrogen) with 11 mM glucose (Sigma), 100 units/ml penicillin, 100 µg/ml streptomycin (Invitrogen), and 10% vol/vol FBS (Invitrogen). Real-time RT-PCR was conducted as described previously (Szabat et al., 2016). A list of primers used can be found in Table S2.

Fluorescence-activated cell sorting

Pancreatic islets were dispersed using 0.005% trypsin and resuspended in 1xPBS with 0.005% FBS. Dispersed islets were then filtered into 5 ml polypropylene tubes. Fluorescence-activated cell sorting was conducted on a Cytopeia Influx sorter (Becton Dickinson, Franklin Lakes, NJ, USA) at the Life Sciences Institute core facility. Cells were excited with a 488□nm laser (530/40 emission) and a 561□nm laser (610/20□emission).

Live-cell imaging

To define the incidence and kinetics of the transitions in *Ins2* gene activity, we will culture dispersed islet cells on 96-well well glass bottom plates, and image them every 30 minutes for up to 48 hours through a 40x air objective using a ImageXpress^{MICRO} environmentally-controlled, robotic imaging system (Molecular Devices)(Yang and Johnson, 2013). Movies were analyzed using Cell Profiler software and custom R scripts.

Live cell imaging of cell death

Our methods for live cell imaging of islet cell survival have been previously published (Yang and Johnson, 2013). Briefly, pancreatic islet cells were dissociated, and cultured in RPMI 1640 media with 10% FBS (Gibco, Fisher Scientific, Gaithersburg, MD, USA), and penicillin/streptomycin on 96 well glass bottom plates for 48 hours. Dispersed islet cells were then exposed to different dose of glucose, as well as thapsigargin (Sigma, St. Louis, MO, USA). Islet cell death was measured by propidium iodide incorporation. Images were taken every 30 min for up to 48 hours, as described earlier. Propidium iodide incorporation was traced throughout the time period, and area under the curve was measured.

Single cell transcriptomics

Single Cell Suspension was loaded on the 10x genomics single cell controller for capture in droplet emulsion. The 60-week old mouse islet cell libraries were prepared using the Chromium Single Cell 3' Reagent v2 Chemistry kit (10x Genomics, Pleasanton, CA, USA) and the standard protocol was followed for all steps. The 8-week old mouse islet cell libraries were prepared using the Chromium Single Cell 3' Reagent v3 Chemistry kit (10x Genomics). Libraries were then sequenced on a Nextseq500 (Illumina). Cell Ranger 2.0 and 3.0 (10x Genomics) were used to perform demultiplexing, alignment, counting, clustering, and differential expression analysis for each cluster for 60-week-old mouse data and 8-week-old mouse data respectively. The analysis results were visualized using 10x Genomics Loupe Cell Browser. Seurat R package (version 2.3.4) was used to process count matrices, generate violin plots and heatmaps (Butler et al., 2018). The cells were labeled as +/- for each marker gene using k-means clustering (k=2). Differential expression analysis between different subsets of cells was performed using the Wilcoxon rank sum test option in Seurat. Differential expression analysis over GFP gradient was performed using monocle R package (version 2.6.4)(Qiu et al., 2017). Gene ontology analysis was performed using DAVID (https://david.ncifcrf.gov/content.jsp?file=citation.htm).

Statistical analysis

Data are shown as mean plus/minus standard error of the mean unless otherwise indicated. Differences between 2 groups were evaluated with Student's t-test and between more than 2 groups using ANOVA, calculated with Prizm software (Graphpad Software, San Diego, CA, USA).

References

Atger, F., Gobet, C., Marquis, J., Martin, E., Wang, J., Weger, B., Lefebvre, G., Descombes, P., Naef, F., and Gachon, F. (2015). Circadian and feeding rhythms differentially affect rhythmic mRNA transcription and translation in mouse liver. Proc Natl Acad Sci U S A *112*, E6579-6588.

Bader, E., Migliorini, A., Gegg, M., Moruzzi, N., Gerdes, J., Roscioni, S.S., Bakhti, M., Brandl, E., Irmler, M., Beckers, J., et al. (2016). Identification of proliferative and mature beta-cells in the islets of Langerhans. Nature *535*, 430-434.

Basford, C.L., Prentice, K.J., Hardy, A.B., Sarangi, F., Micallef, S.J., Li, X., Guo, Q., Elefanty, A.G., Stanley, E.G., Keller, G., et al. (2012). The functional and molecular characterisation of human embryonic stem cell-derived insulin-positive cells compared with adult pancreatic beta cells. Diabetologia *55*, 358-371.

Benner, C., van der Meulen, T., Caceres, E., Tigyi, K., Donaldson, C.J., and Huising, M.O. (2014). The transcriptional landscape of mouse beta cells compared to human beta cells

reveals notable species differences in long non-coding RNA and protein-coding gene expression. BMC Genomics *15*, 620.

Benninger, R.K.P., and Hodson, D.J. (2018). New Understanding of beta-Cell Heterogeneity and In Situ Islet Function. Diabetes *67*, 537-547.

Butler, A., Hoffman, P., Smibert, P., Papalexi, E., and Satija, R. (2018). Integrating single-cell transcriptomic data across different conditions, technologies, and species. Nat Biotechnol *36*, 411-420.

Corish, P., and Tyler-Smith, C. (1999). Attenuation of green fluorescent protein half-life in mammalian cells. Protein Eng *12*, 1035-1040.

Dirice, E., Kahraman, S., De Jesus, D.F., El Ouaamari, A., Basile, G., Baker, R.L., Yigit, B., Piehowski, P.D., Kim, M.J., Dwyer, A.J., et al. (2019). Increased β-cell proliferation before immune cell invasion prevents progression of type 1 diabetes. Nature Metabolism.

Dorrell, C., Schug, J., Canaday, P.S., Russ, H.A., Tarlow, B.D., Grompe, M.T., Horton, T., Hebrok, M., Streeter, P.R., Kaestner, K.H., et al. (2016). Human islets contain four distinct subtypes of beta cells. Nat Commun *7*, 11756.

Farack, L., Golan, M., Egozi, A., Dezorella, N., Bahar Halpern, K., Ben-Moshe, S., Garzilli, I., Toth, B., Roitman, L., Krizhanovsky, V., et al. (2019). Transcriptional Heterogeneity of Beta Cells in the Intact Pancreas. Dev Cell *48*, 115-125 e114.

Harper, C.V., Featherstone, K., Semprini, S., Friedrichsen, S., McNeilly, J., Paszek, P., Spiller, D.G., McNeilly, A.S., Mullins, J.J., Davis, J.R., et al. (2010). Dynamic organisation of prolactin gene expression in living pituitary tissue. J Cell Sci *123*, 424-430.

Heimberg, H., De Vos, A., Vandercammen, A., Van Schaftingen, E., Pipeleers, D., and Schuit, F. (1993). Heterogeneity in glucose sensitivity among pancreatic beta-cells is correlated to differences in glucose phosphorylation rather than glucose transport. Embo J *12*, 2873-2879.

Hrvatin, S., O'Donnell, C.W., Deng, F., Millman, J.R., Pagliuca, F.W., DiIorio, P., Rezania, A., Gifford, D.K., and Melton, D.A. (2014). Differentiated human stem cells resemble fetal, not adult, beta cells. Proc Natl Acad Sci U S A *111*, 3038-3043.

Huang, C., Walker, E.M., Dadi, P.K., Hu, R., Xu, Y., Zhang, W., Sanavia, T., Mun, J., Liu, J., Nair, G.G., et al. (2018). Synaptotagmin 4 Regulates Pancreatic beta Cell Maturation by Modulating the Ca(2+) Sensitivity of Insulin Secretion Vesicles. Dev Cell *45*, 347-361 e345.

Johnson, J.D. (2016). The quest to make fully functional human pancreatic beta-cells from embryonic stem cells: Climbing a mountain in the clouds. Diabetologia *59*, 2047-2057.

Johnson, J.D., Ahmed, N.T., Luciani, D.S., Han, Z., Tran, H., Fujita, J., Misler, S., Edlund, H., and Polonsky, K.S. (2003). Increased islet apoptosis in Pdx1+/- mice. J Clin Invest *111*, 1147-1160.

Johnson, J.D., Bernal-Mizrachi, E., Alejandro, E.U., Han, Z., Kalynyak, T.B., Li, H., Beith, J.L., Gross, J., Warnock, G.L., Townsend, R.R., et al. (2006). Insulin protects islets from apoptosis via Pdx1 and specific changes in the human islet proteome. Proc Natl Acad Sci U S A *103*, 19575-19580.

Johnston, N.R., Mitchell, R.K., Haythorne, E., Pessoa, M.P., Semplici, F., Ferrer, J., Piemonti, L., Marchetti, P., Bugliani, M., Bosco, D., et al. (2016). Beta Cell Hubs Dictate Pancreatic Islet Responses to Glucose. Cell Metab *24*, 389-401.

Katsuta, H., Aguayo-Mazzucato, C., Katsuta, R., Akashi, T., Hollister-Lock, J., Sharma, A.J., Bonner-Weir, S., and Weir, G.C. (2012). Subpopulations of GFP-marked mouse pancreatic beta-cells differ in size, granularity, and insulin secretion. Endocrinology *153*, 5180-5187.

Kiekens, R., In 't Veld, P., Mahler, T., Schuit, F., Van De Winkel, M., and Pipeleers, D. (1992). Differences in glucose recognition by individual rat pancreatic B cells are associated with intercellular differences in glucose-induced biosynthetic activity. J Clin Invest *89*, 117-125.

Kolic, J., and Johnson, J.D. (2016). Specialized Hub Beta Cells Trade Maximal Insulin Production for Perfect Timing. Cell Metab *24*, 371-373.

Leroux, L., Desbois, P., Lamotte, L., Duvillie, B., Cordonnier, N., Jackerott, M., Jami, J., Bucchini, D., and Joshi, R.L. (2001). Compensatory responses in mice carrying a null mutation for Ins1 or Ins2. Diabetes *50 Suppl 1*, S150-153.

Ling, Z., Chen, M.C., Smismans, A., Pavlovic, D., Schuit, F., Eizirik, D.L., and Pipeleers, D.G. (1998). Intercellular differences in interleukin 1beta-induced suppression of insulin synthesis and stimulation of noninsulin protein synthesis by rat pancreatic beta-cells. Endocrinology *139*, 1540-1545.

Mehran, A.E., Templeman, N.M., Brigidi, G.S., Lim, G.E., Chu, K.Y., Hu, X., Botezelli, J.D., Asadi, A., Hoffman, B.G., Kieffer, T.J., et al. (2012). Hyperinsulinemia drives diet-induced obesity independently of brain insulin production. Cell Metab *16*, 723-737.

Molina, N., Suter, D.M., Cannavo, R., Zoller, B., Gotic, I., and Naef, F. (2013). Stimulus-induced modulation of transcriptional bursting in a single mammalian gene. Proc Natl Acad Sci U S A *110*, 20563-20568.

Nakayama, M., Abiru, N., Moriyama, H., Babaya, N., Liu, E., Miao, D., Yu, L., Wegmann, D.R., Hutton, J.C., Elliott, J.F., et al. (2005). Prime role for an insulin epitope in the development of type 1 diabetes in NOD mice. Nature *435*, 220-223.

Nicolas, D., Phillips, N.E., and Naef, F. (2017). What shapes eukaryotic transcriptional bursting? Mol Biosyst *13*, 1280-1290.

Nicolas, D., Zoller, B., Suter, D.M., and Naef, F. (2018). Modulation of transcriptional burst frequency by histone acetylation. Proc Natl Acad Sci U S A *115*, 7153-7158.

Norris, A.J., Stirland, J.A., McFerran, D.W., Seymour, Z.C., Spiller, D.G., Loudon, A.S., White, M.R., and Davis, J.R. (2003). Dynamic patterns of growth hormone gene transcription in individual living pituitary cells. Mol Endocrinol *17*, 193-202.

Perl, S., Kushner, J.A., Buchholz, B.A., Meeker, A.K., Stein, G.M., Hsieh, M., Kirby, M., Pechhold, S., Liu, E.H., Harlan, D.M., et al. (2010). Significant human beta-cell turnover is limited to the first three decades of life as determined by in vivo thymidine analog incorporation and radiocarbon dating. J Clin Endocrinol Metab *95*, E234-239.

Phillips, N.E., Mandic, A., Omidi, S., Naef, F., and Suter, D.M. (2019). Memory and relatedness of transcriptional activity in mammalian cell lineages. Nat Commun *10*, 1208.

Pichon, X., Lagha, M., Mueller, F., and Bertrand, E. (2018). A Growing Toolbox to Image Gene Expression in Single Cells: Sensitive Approaches for Demanding Challenges. Mol Cell *71*, 468-480.

Pipeleers, D.G. (1992). Heterogeneity in pancreatic beta-cell population. Diabetes *41*, 777-781.

Qiu, X., Mao, Q., Tang, Y., Wang, L., Chawla, R., Pliner, H.A., and Trapnell, C. (2017). Reversed graph embedding resolves complex single-cell trajectories. Nat Methods *14*, 979-982.

Raj, A., Peskin, C.S., Tranchina, D., Vargas, D.Y., and Tyagi, S. (2006). Stochastic mRNA synthesis in mammalian cells. PLoS Biol *4*, e309.

Rankin, M.M., and Kushner, J.A. (2009). Adaptive beta-cell proliferation is severely restricted with advanced age. Diabetes *58*, 1365-1372.

Rui, J., Deng, S., Arazi, A., Perdigoto, A.L., Liu, Z., and Herold, K.C. (2017). beta Cells that Resist Immunological Attack Develop during Progression of Autoimmune Diabetes in NOD Mice. Cell Metab *25*, 727-738.

Sachdeva, M.M., Claiborn, K.C., Khoo, C., Yang, J., Groff, D.N., Mirmira, R.G., and Stoffers, D.A. (2009). Pdx1 (MODY4) regulates pancreatic beta cell susceptibility to ER stress. Proc Natl Acad Sci U S A *106*, 19090-19095.

Segerstolpe, A., Palasantza, A., Eliasson, P., Andersson, E.M., Andreasson, A.C., Sun, X., Picelli, S., Sabirsh, A., Clausen, M., Bjursell, M.K., et al. (2016). Single-Cell Transcriptome Profiling of Human Pancreatic Islets in Health and Type 2 Diabetes. Cell Metab *24*, 593-607.

Stadinski, B.D., Delong, T., Reisdorph, N., Reisdorph, R., Powell, R.L., Armstrong, M., Piganelli, J.D., Barbour, G., Bradley, B., Crawford, F., et al. (2010). Chromogranin A is an autoantigen in type 1 diabetes. Nat Immunol *11*, 225-231.

Suter, D.M., Molina, N., Gatfield, D., Schneider, K., Schibler, U., and Naef, F. (2011). Mammalian genes are transcribed with widely different bursting kinetics. Science *332*, 472-474.

Szabat, M., Johnson, J.D., and Piret, J.M. (2010). Reciprocal modulation of adult beta cell maturity by activin A and follistatin. Diabetologia *53*, 1680-1689.

Szabat, M., Luciani, D.S., Piret, J.M., and Johnson, J.D. (2009). Maturation of adult beta-cells revealed using a Pdx1/insulin dual-reporter lentivirus. Endocrinology *150*, 1627-1635.

Szabat, M., Lynn, F.C., Hoffman, B.G., Kieffer, T.J., Allan, D.W., and Johnson, J.D. (2012). Maintenance of beta-cell maturity and plasticity in the adult pancreas: developmental biology concepts in adult physiology. Diabetes *61*, 1365-1371.

Szabat, M., Page, M.M., Panzhinskiy, E., Skovso, S., Mojibian, M., Fernandez-Tajes, J., Bruin, J.E., Bround, M.J., Lee, J.T., Xu, E.E., et al. (2016). Reduced Insulin Production Relieves Endoplasmic Reticulum Stress and Induces beta Cell Proliferation. Cell Metab *23*, 179-193.

Szabat, M., Pourghaderi, P., Soukhatcheva, G., Verchere, C.B., Warnock, G.L., Piret, J.M., and Johnson, J.D. (2011). Kinetics and genomic profiling of adult human and mouse beta-cell maturation. Islets *3*, 175-187.

Teta, M., Long, S.Y., Wartschow, L.M., Rankin, M.M., and Kushner, J.A. (2005). Very slow turnover of beta-cells in aged adult mice. Diabetes *54*, 2557-2567.

Thomsen, S.K., Raimondo, A., Hastoy, B., Sengupta, S., Dai, X.Q., Bautista, A., Censin, J., Payne, A.J., Umapathysivam, M.M., Spigelman, A.F., et al. (2018). Type 2 diabetes risk alleles in PAM impact insulin release from human pancreatic beta-cells. Nat Genet *50*, 1122-1131.

van der Meulen, T., Mawla, A.M., DiGruccio, M.R., Adams, M.W., Nies, V., Dolleman, S., Liu, S., Ackermann, A.M., Caceres, E., Hunter, A.E., et al. (2017). Virgin Beta Cells Persist throughout Life at a Neogenic Niche within Pancreatic Islets. Cell Metab *25*, 911-926 e916.

Vera, M., Biswas, J., Senecal, A., Singer, R.H., and Park, H.Y. (2016). Single-Cell and Single-Molecule Analysis of Gene Expression Regulation. Annual review of genetics *50*, 267-291.

Veres, A., Faust, A.L., Bushnell, H.L., Engquist, E.N., Kenty, J.H., Harb, G., Poh, Y.C., Sintov, E., Gurtler, M., Pagliuca, F.W., et al. (2019). Charting cellular identity during human in vitro beta-cell differentiation. Nature *569*, 368-373.

Wakae-Takada, N., Xuan, S., Watanabe, K., Meda, P., and Leibel, R.L. (2013). Molecular basis for the regulation of islet beta cell mass in mice: the role of E-cadherin. Diabetologia *56*, 856-866.

Walsh, H.E., and Shupnik, M.A. (2009). Proteasome regulation of dynamic transcription factor occupancy on the GnRH-stimulated luteinizing hormone beta-subunit promoter. Mol Endocrinol *23*, 237-250.

Wenzlau, J.M., Juhl, K., Yu, L., Moua, O., Sarkar, S.A., Gottlieb, P., Rewers, M., Eisenbarth, G.S., Jensen, J., Davidson, H.W., et al. (2007). The cation efflux transporter ZnT8 (Slc30A8) is a major autoantigen in human type 1 diabetes. Proc Natl Acad Sci U S A *104*, 17040-17045.

Wills, Q.F., Boothe, T., Asadi, A., Ao, Z., Warnock, G.L., Kieffer, T.J., and Johnson, J.D. (2016). Statistical approaches and software for clustering islet cell functional heterogeneity. Islets *8*, 48-56.

Xin, Y., Dominguez Gutierrez, G., Okamoto, H., Kim, J., Lee, A.H., Adler, C., Ni, M., Yancopoulos, G.D., Murphy, A.J., and Gromada, J. (2018). Pseudotime Ordering of Single Human beta-Cells Reveals States of Insulin Production and Unfolded Protein Response. Diabetes *67*, 1783-1794.

Yang, B.T., Dayeh, T.A., Kirkpatrick, C.L., Taneera, J., Kumar, R., Groop, L., Wollheim, C.B., Nitert, M.D., and Ling, C. (2011). Insulin promoter DNA methylation correlates negatively with insulin gene expression and positively with HbA(1c) levels in human pancreatic islets. Diabetologia *54*, 360-367.

Yang, Y.H., and Johnson, J.D. (2013). Multi-parameter single-cell kinetic analysis reveals multiple modes of cell death in primary pancreatic beta-cells. J Cell Sci *126*, 4286-4295.

Figure Legends

Figure 1. *In vivo* heterogeneity of insulin content and gene activity in human and mouse islets. (A) Variability in insulin and PDX1 protein levels in human pancreatic β-cells *in vivo*. Scale bar is 20 μm. **(B)** The *Ins2*$^{GFP/GFP}$ knock-in mouse model. Illustration shows, so scale, the replacement of most of the second exon with wildtype GFP. The wildtype *Ins2* locus is shown for comparison, including RNA-seq exon coverage, aggregate (filtered) from NCBI *Mus musculus* Annotation release 106 (log 2 base scaled). **(C)** Normal glucose homeostasis in *Ins2*$^{GFP/Wt}$;*Ins2*$^{GFP/GFP}$ mice and WT (Male n=3-7, Female n=3-4). **(D)** GFP from the endogenous *Ins2* gene locus is high in a subset of mouse pancreatic β-cells. Scale bar is 20 μm. **(E)** Detection of *Ins2*(GFP)^{LOW} and *Ins2*(GFP)^{HIGH} populations of β-cells by FACS. **(F,G)** GFP mRNA and *Ins2* mRNA in *Ins2*$^{GFP/Wt}$ and *Ins2*$^{GFP/GFP}$ cells. FACS purification of cells that are negative (-) or positive (+) for GFP fluorescence relative to the background fluorescence of C57Bl6J wildtype control islets. (**H**) Presumed transcription-to-maturation times of GFP and insulin. See Supplemental Information for calculations and references.

Figure 2. Tracking β-cell heterogeneity with *Ins1*-mCherry;*Ins2*$^{GFP/GFP}$ knock-in mice. (A) Experimental model for tracking activity at the endogenous *Ins2* locus (GFP) in β-cells marked with mCherry driven by an *Ins1* promoter, which constitutively marks 98% of β-cells. Scale bar is 50 μm **(B)** Live-cell imaging of islet cells isolated and dispersed from *Ins1*-mCherry;*Ins2*$^{GFP/wt}$ mice. Scale bar is 50 μm. **(C,D)** Distinct populations of *Ins2*(GFP)^{LOW} β-cells and *Ins2*(GFP)^{HIGH} β-cells were FACS purified and examined by qPCR for *gfp*, *Ins2*, pre-*Ins2*, *Ins1* and pre-*Ins1* mRNA (n=3).

Figure 3. Live-cell imaging *Ins2* gene activity reveals bursting behavior of the endogenous *Ins2* gene locus. (A) Dynamic imaging, over 30 hours in culture, of dispersed islet cells from *Ins1*-mCherry;*Ins2*$^{GFP/GFP}$ mice labelled with Hoechst vital nuclear dye. Note the examples of cells with bursting GFP fluorescence. Scale bar is 50 μm. **(B,C)** Clustering of cellular *Ins2* gene activity (GFP) dynamics and mCherry dynamics based on 16 parameters leads to 3 cellular behaviour groupings. Parameters included oscillations, (full width at half maximum) FWHM, mean, AUC, and shape (as marker of sharp peaks). **(D)** Examples of 3 cellular behaviour groupings are shown.

Figure 4. Single-cell RNA sequencing analysis of *Ins2*(GFP)^{LOW} and *Ins2*(GFP)^{HIGH} β-cells in young mice. (A) t-SNE plot of all cells positive for *Ins1* mRNA (β-cells) isolated and dispersed from *Ins2*$^{GFP/wt}$ mice FACS purified into either GFP-negative (-) or GFP-positive (+) groups. **(B)** *Ins1, Ins2,* and *gfp* mRNA quantification distributions from GFP-negative or GFP-positive single β-cells. **(C)** Gene Ontology Categories that are driven by genes differentially expressed in *Ins2*(GFP)^{LOW} versus *Ins2*(GFP)^{HIGH} β-cells. **(D)** Individual genes that are differentially expressed as a function of *gfp* mRNA expression.

Figure 5. Single-cell RNA sequencing analysis of *Ins2*(GFP)^{LOW} and *Ins2*(GFP)^{HIGH} β-cells in old mice. (A) t-SNE plot of all cells positive for *Ins1* mRNA (β-cells) isolated and dispersed from *Ins2*$^{GFP/wt}$ or *Ins2*$^{GFP/GFP}$ mice FACS purified into either GFP-negative (-) or GFP-positive (+) groups. **(B)** *Ins1, Ins2,* and *gfp* mRNA quantification distributions from GFP-negative or GFP-positive single β-cells. **(C)** Gene Ontology categories that are driven by genes differentially expressed in *Ins2*(GFP)^{LOW} versus *Ins2*(GFP)^{HIGH} β-cells. **(D)** Individual genes that are differentially expressed as a function of *gfp* mRNA expression.

Figure 6. *Ins2*(GFP)^{HIGH} β-cells show increased cell death across multiple conditions. (A) GFP-positive cells show increased apoptosis susceptibility at all tested glucose concentrations and in the presence of thapsigargin (>1000 cells/condition, repeated from 2 mice). **(B)** Working model of a hypothetical β-cell bursting cycle.

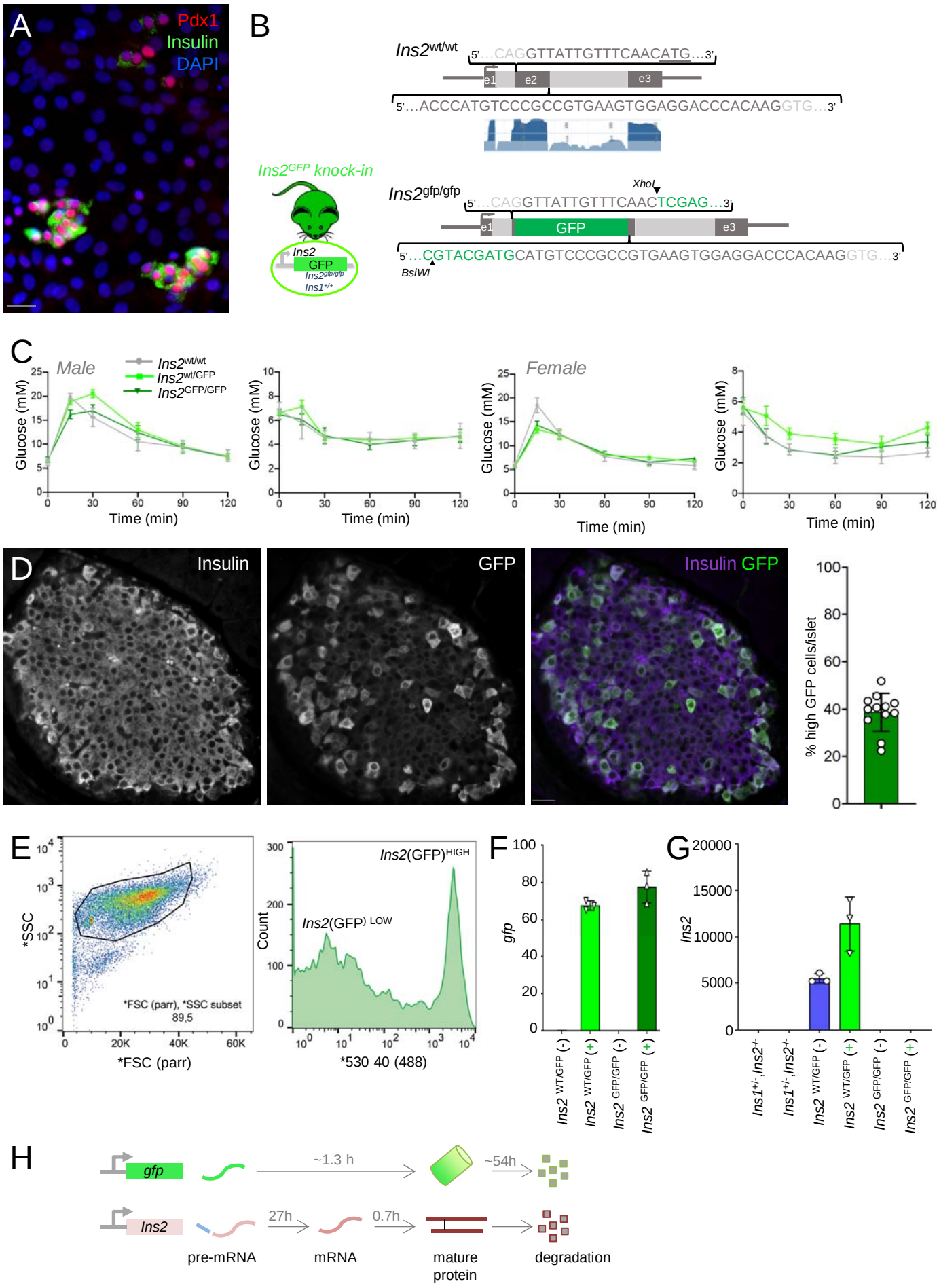

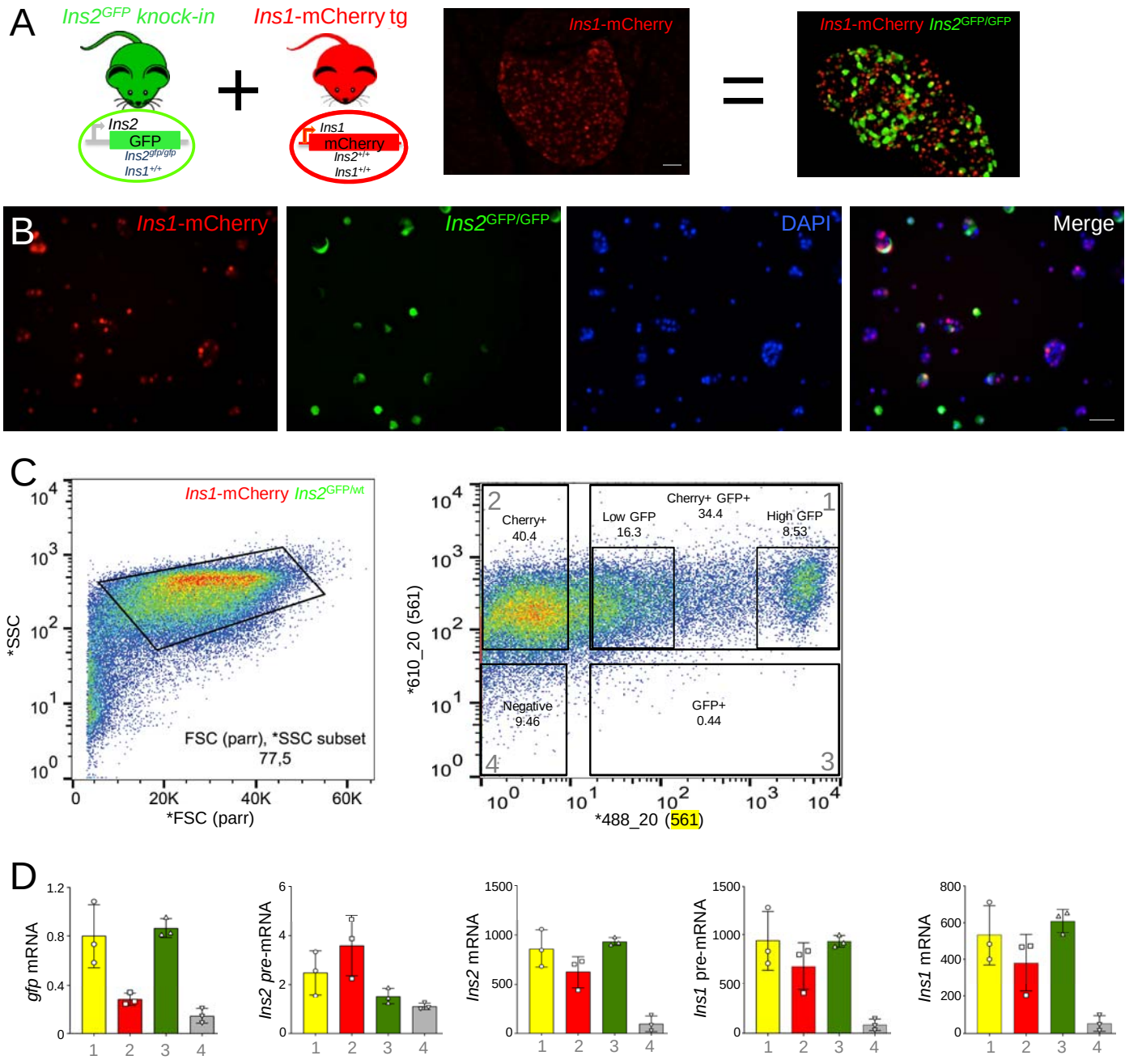

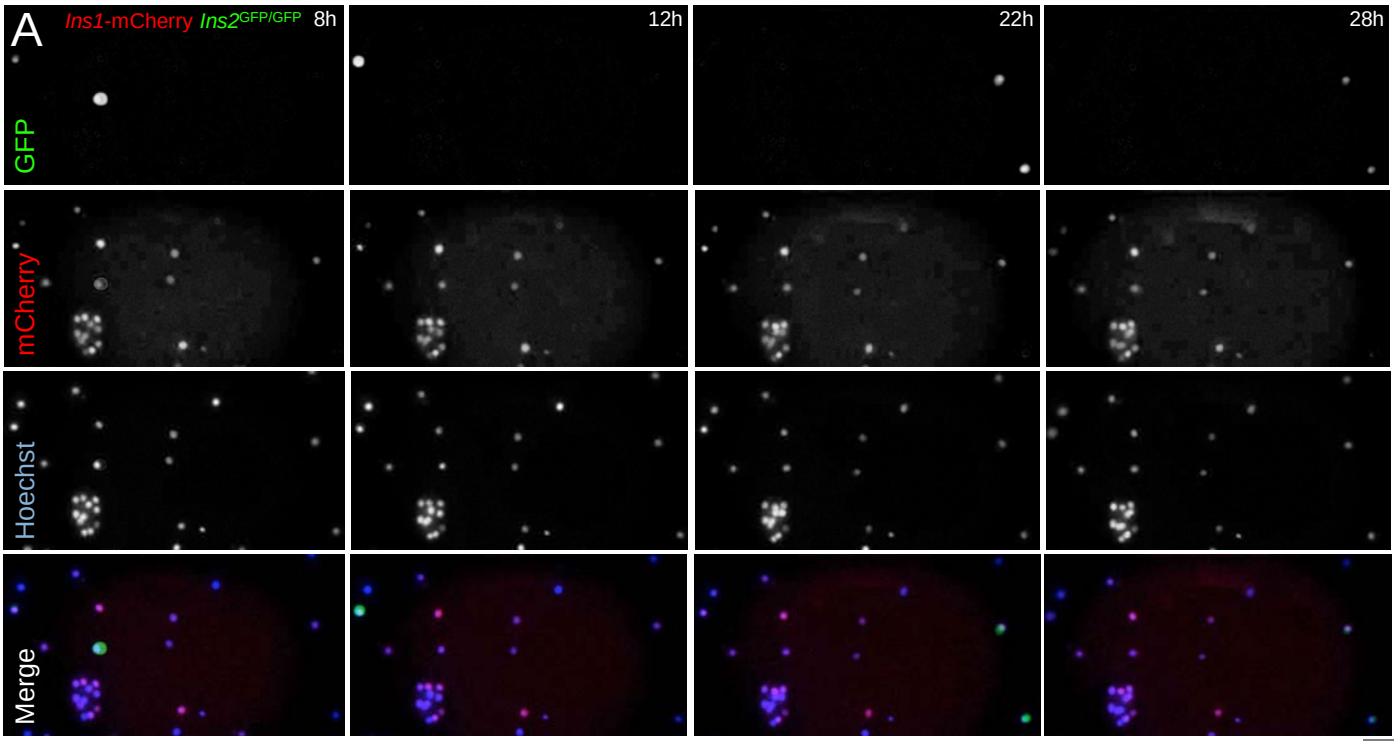

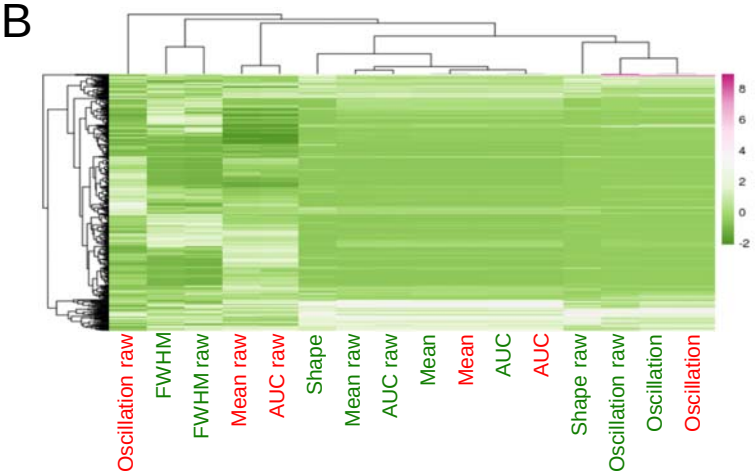

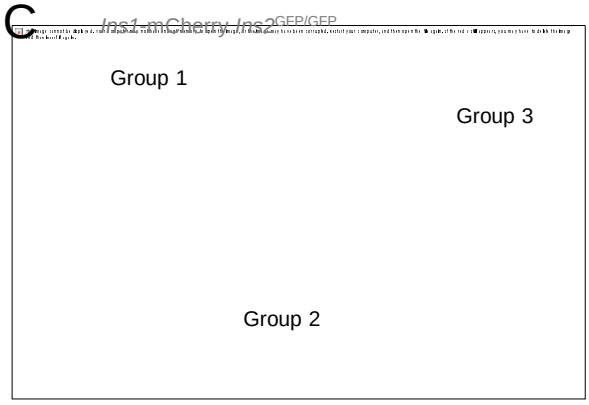

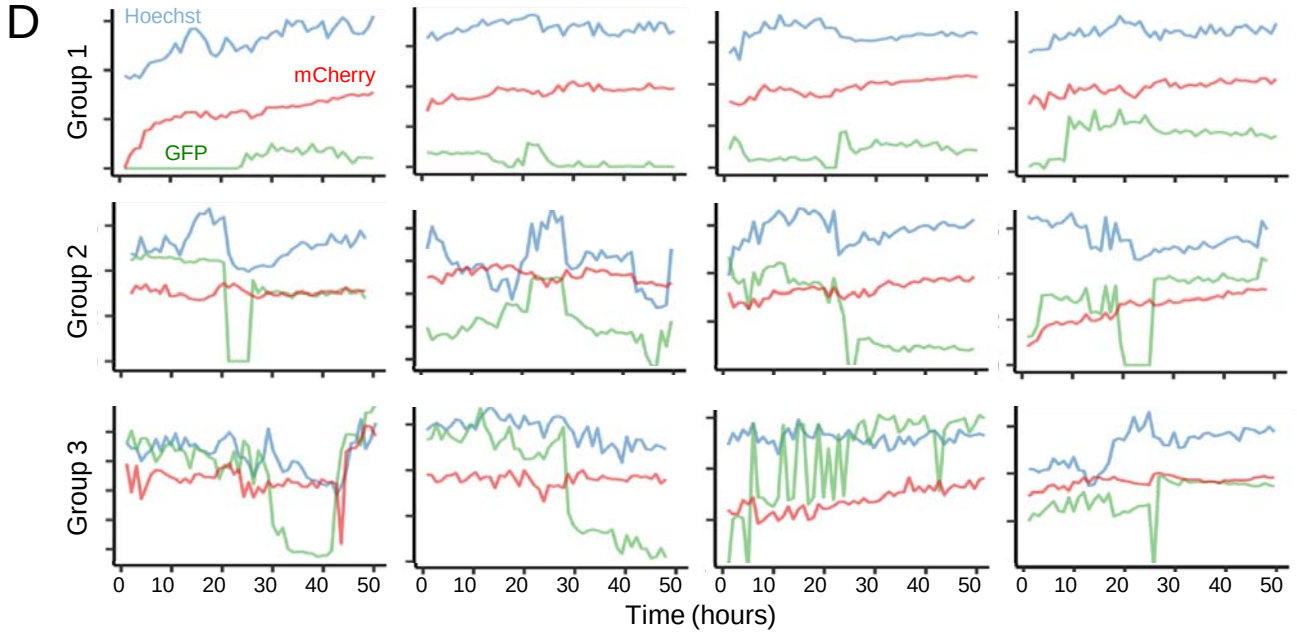

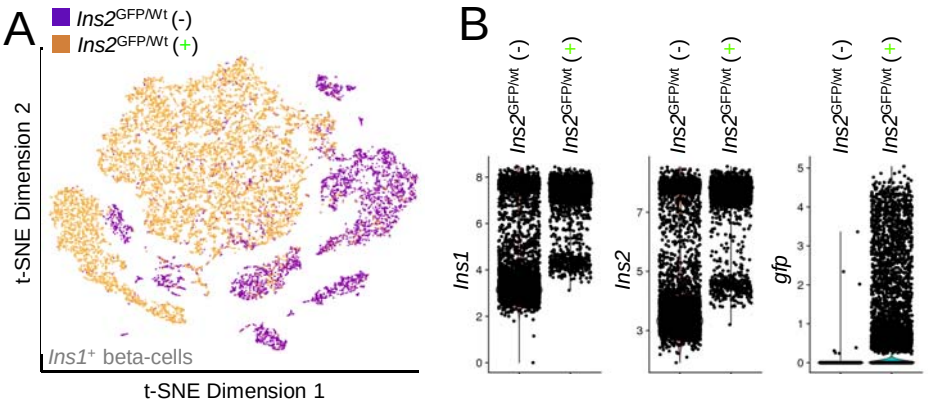

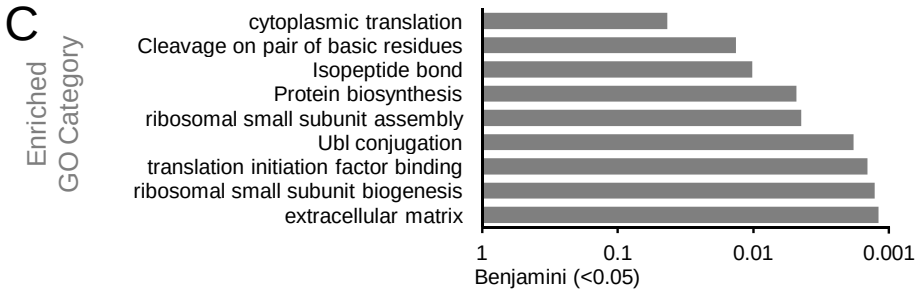

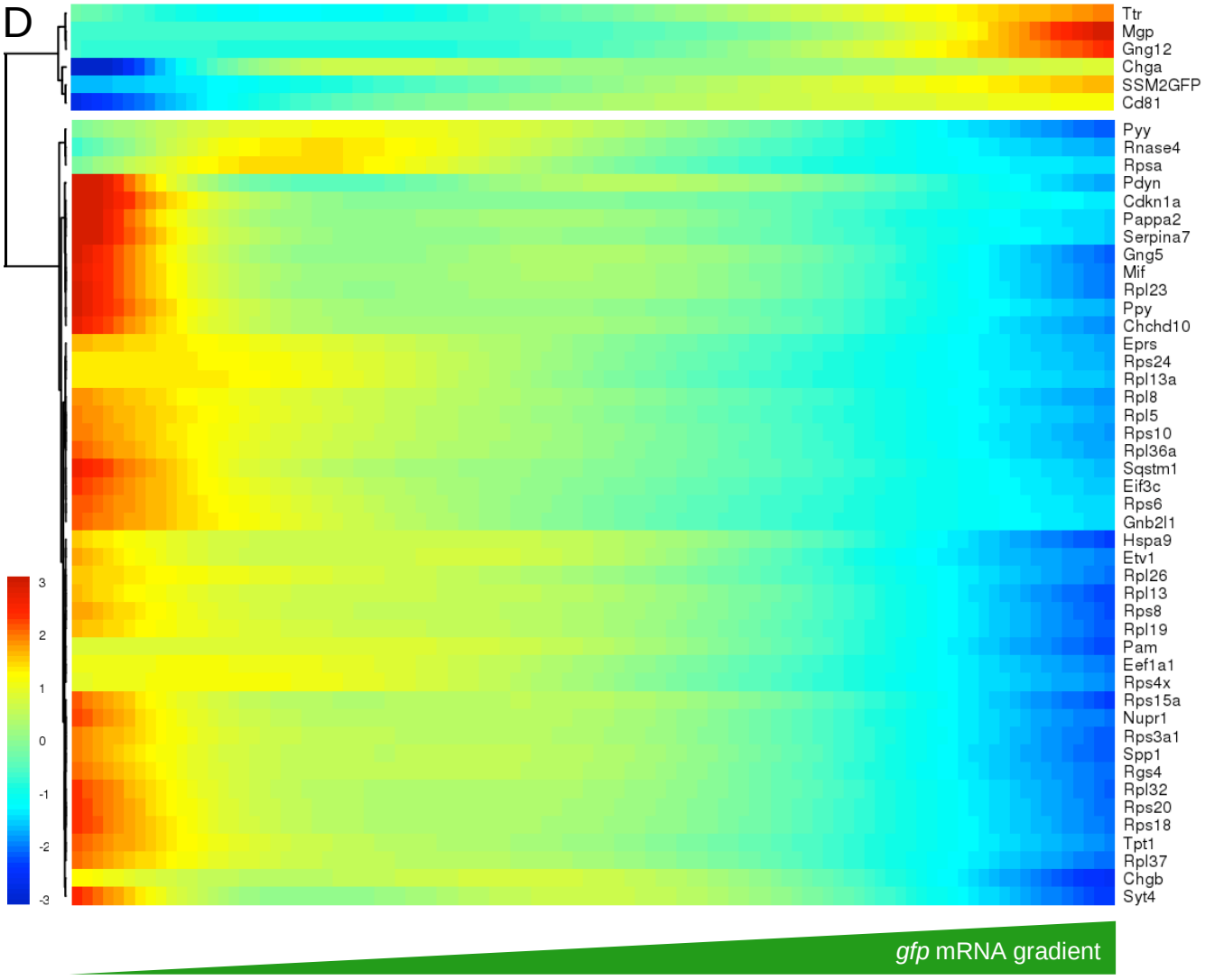

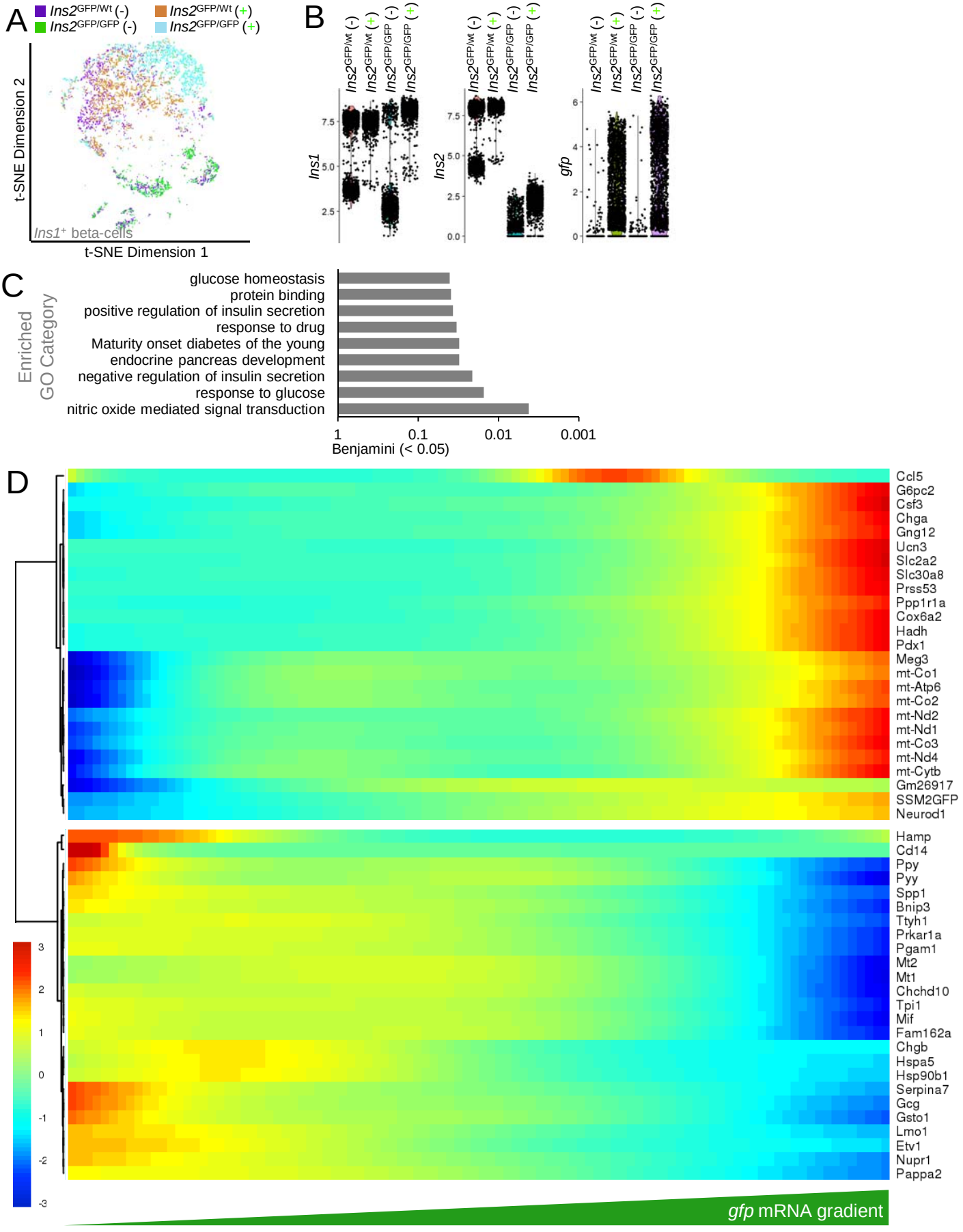

A

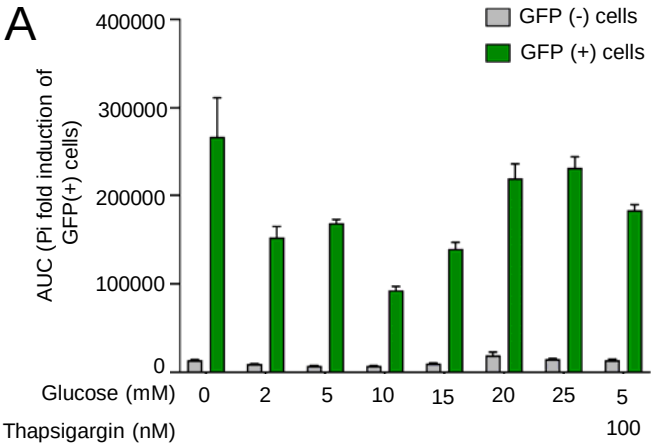

B